A mineralogical, fluid inclusion, and isotopic study of selected epithermal Ag-Au occurrences in the Banská Štiavnica–Hodruša-Hámre ore district, Western Carpathians

Juraj Majzlan[1], Khulan Berkh[1], Peter Koděra[2], Martin Števko[3], František Bakos[4] & Rastislav Milovský[5]

[1]Institute of Geosciences, Friedrich-Schiller University, Carl-Zeiss Promenade 10, D-07745 Jena, Germany; Juraj.Majzlan@uni-jena.de
[2]Department of Geology of Mineral Deposits, Faculty of Natural Sciences, Comenius University, Ilkovičova 6, 842 15 Bratislava, Slovakia
[3]Department of Mineralogy and Petrology, Faculty of Natural Sciences, Comenius University, Ilkovičova 6, 842 15 Bratislava, Slovakia
[4]Green View, Nevädzová 5, 821 01 Bratislava, Slovakia
[5]Earth Science Institute, Slovak Academy of Sciences, Ďumbierska 1, 974 01 Banská Bystrica, Slovakia

AGEOS

Výskum mineralógie, fluidných inklúzií a stabilných izotopov na vybraných epitermálnych Ag-Au výskytoch v banskoštiavnickom-hodrušskom rudnom poli v Západných Karpatoch

Abstract: Here we present new data for samples from Treiboltz, Rabenstein, Bursa, Trojkráľová, and Schöpfer, all occurrences of epithermal ores in the Banská Štiavnica-Hodruša-Hámre ore district. The ores at Treiboltz and Rabenstein are simple hydrothermal breccias or silicified zones. The breccias contain strongly altered lithoclasts, the ore-bearing quartz, and latest drusy quartz. Fluid inclusions were found only in the late quartz, with salinities of 1.5-5.5 wt.% NaCl eq. and homogenization temperatures between 200-300 °C. The drillhole samples from Bursa contain only weak base-metal mineralization (pyrite, galena, sphalerite, chalcopyrite). Fluid inclusions were measured in quartz that is likely associated with sulfide precipitation and late calcite that fills cavities in the ores. All these inclusions have similar salinity and homogenization temperature ranges as those reported for Treiboltz and Rabenstein. Rich ore samples from the Schöpfer vein, one of the largest ore veins in Hodruša-Hámre, revealed astonishing complexity at microscale. They show growth of minerals into open space in a dynamic environment, with frequent changes between precipitation of quartz and carbonate (mostly Mn-calcite) and pseudomorphs of quartz after bladed calcite. Adularia is also common in some zones. The ores comprise base-metal minerals and abundant polybasite-pearceite and electrum. Unusual chemical variability of carbonates associated with the ores could be a sign of sudden fluid change prior to ore precipitation. Fluid inclusions measured in different types of quartz and calcite gave salinities of 1.0-5.5 wt.% NaCl eq. and homogenization temperatures mostly between 200-300 °C. Calculated isotopic composition of the fluids suggest large proportion of meteoric waters in these fluids.

Key words: epithermal veins, Banská Štiavnica-Hodruša, mineralogy, fluid inclusions, stable isotopes

1. INTRODUCTION

The Banská Štiavnica-Hodruša-Hámre ore district yielded approximately 80 tons of Au and 4000 tons of Ag during the last 400 years (Lexa et al., 1999). Precious-metal mining ceased in 1947 and the base-metal mines shut down in 1992. Deep gold ores, discovered by a lucky coincidence in the late 1980's (Koděra et al., 2014), secured the continuation of mining in the last gold mine in central Europe until today. Mining of the traditional Ag-Au ores, explored perhaps over 2000 years, was not revived. Given the historical importance of these ores and the potential to locate new reserves, the Ag-Au ores deserve scientific attention, in addition to the current exploration efforts in this area.

The evolution of the stratovolcano, together with the corresponding ore-forming processes in each stage, were described in detail by Lexa et al. (1999). For the sites studied here, only the last stages of the evolution, so-called post-caldera stage, and the associated fluids, are relevant. The epithermal mineralization, however, can be hosted by older volcanic rocks or even rocks of the pre-volcanic basement. The initial stages of the stratovolcano evolution produced large quantities of pyroxene and amphibole-pyroxene andesites, followed by emplacement of a diorite pluton. A later emplacement of a large, bell-jar body of granodiorite caused the formation of small Fe-skarn bodies and base metal stockwork mineralisation. Later injections of granodiorite and quartz diorite porphyry stocks are responsible for some Cu-Au porphyry systems in the studied area. The following caldera collapse was accompanied by emplacement of quartz diorite porphyry sills and dykes and deposition of lacustrine sediments in the caldera. Final stages saw renewed andesitic volcanism, followed by a resurgent horst uplift in the center of the caldera, which was accompanied by rhyolitic volcanic activity. The entire evolution of the Štiavnica stratovolcano occured in the interval 15.0–11.4 Ma (Chernyshev et al., 2013).

The intermediate to low-sulfidation epithermal Ag-Au veins were formed during the early stages of the caldera subsidence (13.1

Manuscript received: 2016-08-30
Revised version accepted: 2016-12-05

-12.7 Ma) and later during the long-lasting horst uplift, dated to 12.2– 10.7 Ma (Lexa et al., 1999; Chernyshev et al., 2013). The later system of veins is extensive with a large historical production of precious and base metal ores. These veins appear in zonal arrangement with three types of veins. Sulphide-rich base metal veins occur in E, SE and central part of the horst, Ag-rich veins (Au:Ag 1:100) are present in central, W and NW part of the horst and low sulfidation Au-rich veins (Au:Ag 1:1 to 1:10) occur on marginal parts of the horst, associated with ryolites (Lexa et al., 1999). Mineralogical composition and the temporal relationships of the minerals in the veins were studied mostly by Koděra (1959, 1960, 1969), Kovalenker et al. (2006) and Onačila et al. (1993). Partial results from selected localities were also reported by Majzlan (2009) and Berkh et al. (2014). Further details and references on the evolution of the caldera, horst, timing of the magmatic and tectonic events, and their coincidence with different mineralization types can be found in Koděra et al. (2005, 2014).

Here, we bring new data on fluid inclusions and mineralogy from epithermal Ag-Au mineralizations Rabenstein, Treiboltz, the vein Schöpfer in Hodruša-Hámre (Ag-rich veins), Bursa veins in eastern margin of Banská Štiavnica and the vein Trojkráľová at the western termination of the Hodruša ore field (Au-rich veins). The mineralogy of the ores from Rabenstein, Treiboltz was already described in our previous contribution (Berkh et al., 2014), and mineralogy of the Trojkráľová vein was described by Štohl et al. (1986) and Onačila and Rojkovičová (1989). Their results will be briefly summarized below. Detailed information about the mineralogy will be presented only for the samples from Schöpfer and Bursa veins.

1.1 General description of the studied sites

The locality Rabenstein belongs to the system of Jozef and Umbruch veins in the easternmost margin of the Hodruša-Hámre ore district (Fig. 1). Rabenstein is a vein in the hanging wall of the Jozef vein, referred to also as the Jozef Rabenstein vein, mined probably in the 15th and 16th century (Kaňa et al., 2011). These veins here are located in strongly altered granodiorite and are associated with massive silicified zones. One such zone forms a marked morphological feature at Rabenstein, elevating several meters above the altered country rocks. The entire zone is made of massive or porous quartz with altered fragments of the country rocks.

The locality Treiboltz is located near a morphologically marked silicified zone with coordinates 48°28'37.962"N and

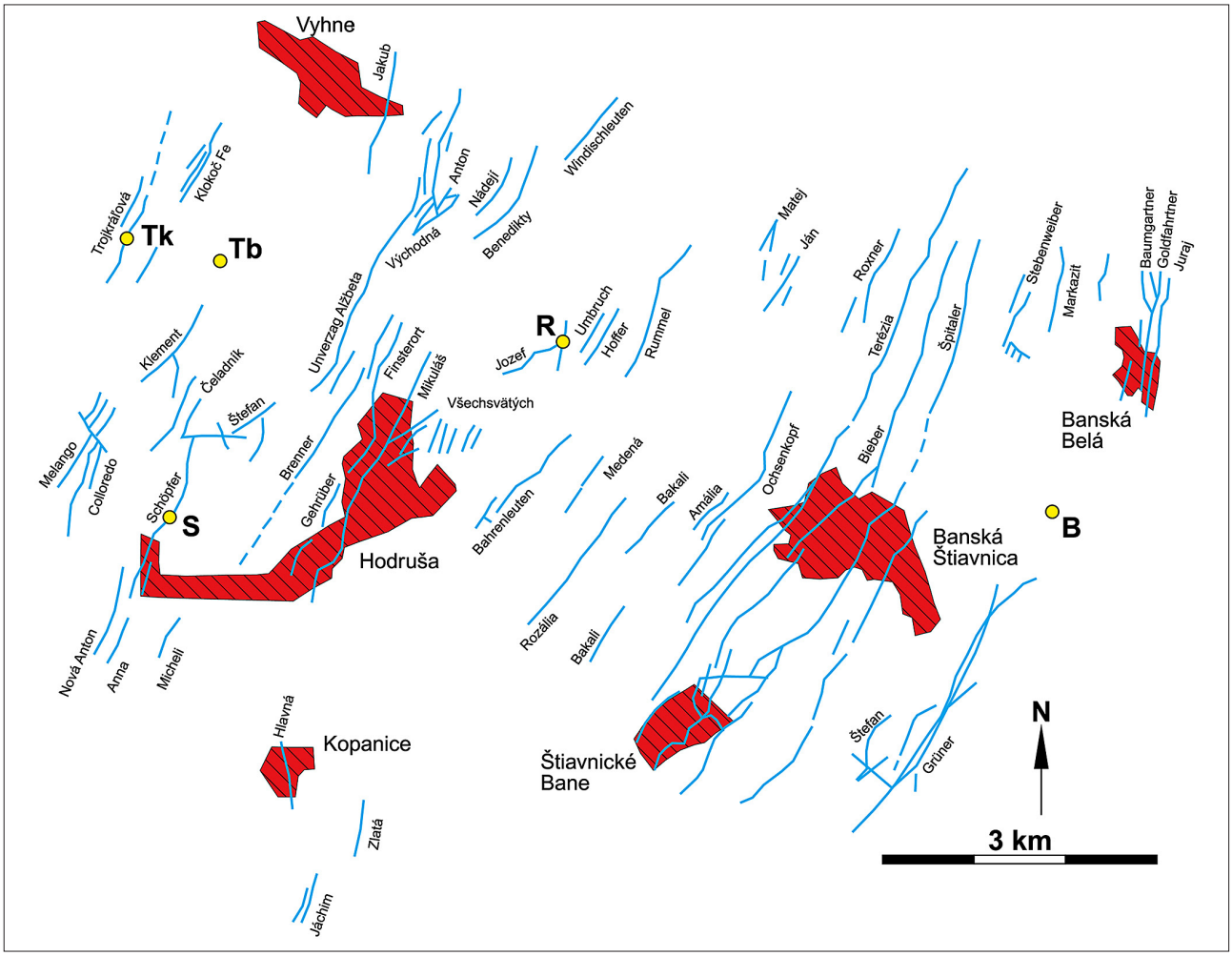

Fig. 1. An overview map of the known ore veins in the broader area of Banská Štiavnica, Hodruša, Vyhne, and Banská Belá (simplified after Bakos et al. 2004). The localities studied are shown by small circles: Tb – Treiboltz, Tk – Trojkráľová, R – Rabenstein, B – Bursa, S – Schöpfer.

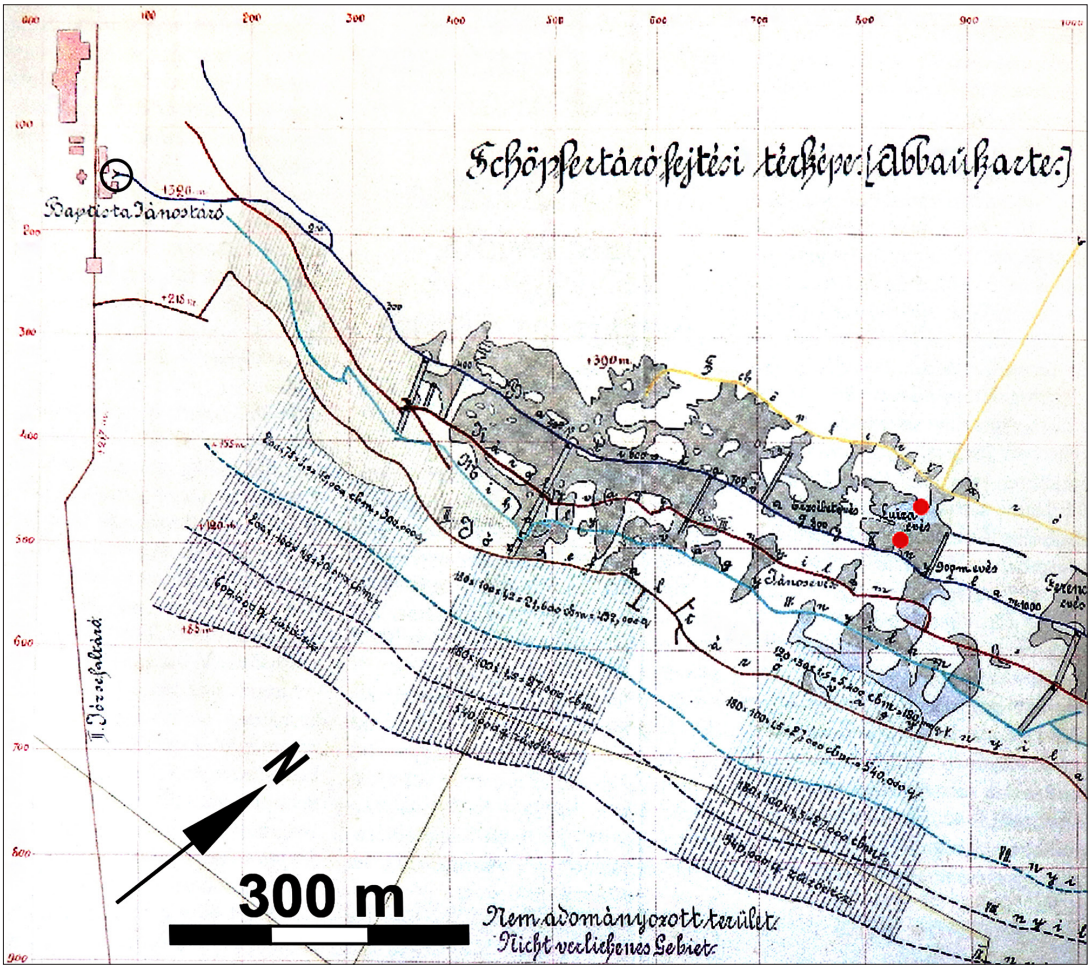

Fig. 2. Sampling points for the primary ores in the Ján Baptista adit, from the Ag-rich Schöpfer vein in Hodruša. A portion of the historical map was taken from Kaňa et al. (2011). Sampling points are shown by small red circles. The open circle with black outline points at the main entrance of the Ján Baptista adit. The color-coded lines represent projections of the levels of the mine onto the surface. Grey-shaded areas are mined out spaces.

18°47'24.272"E. The coordinates listed in Berkh et al. (2014) are incorrect. The site is located about 700 m WNW from the chapel near the elevation point Kerling (820 m.a.s.l.) in Hodruša-Hámre. The silicified wall, similar to the one at Rabenstein, elevates above the soft relief and forms a marked geomorphological feature. It is built by very fine-grained, barren quartz. Ore samples can be located at the dumps of old abandoned mines near the silicified wall. The ore mineralization may belong to the northern extension of the Klement vein or it may represent separate structures.

The Schöpfer vein was one of the largest and most productive veins in the Hodruša-Hámre ore field (Bergfest, 1954; Kaňa et al., 2011). It is hosted by granodiorite and quartz-diorite porphyry, fragmented by younger tectonics, 8-10 meters, exceptionally up to 20 meters thick, mined from Medieval times until 1950. Length of the vein was 3 km and it was mined into the depth of ~450 m.

The Trojkráľová vein is located at the westernmost margin of the ore field (Fig. 1), hosted by strongly altered amphibole-biotite andesites but also basement dolomites and limestones (Onačila et al., 1993). They reported the presence of pyrite, chalcopyrite, galena, sphalerite, tetrahedrite, electrum, and Ag sulfides and sulfosalts. The vein was exploited for gold enclosed in pyrite or disseminated in silicified host rocks. Exploitation ceased in 1860.

There is little known about the Bursa vein-veinlet system. The veins were explored or exploited in the Medieval times by shallow surface pits which were destroyed during the 20th century as the land was used for pasture and agricultural purposes. The mineralized zone is parallel with the Grüner vein, located eastward from the Kalvária hill and Grüner vein in Banská Štiavnica and westward from the Baumgartner-Goldfahrtner vein system in Banská Belá. The weak mineralization is developed in the andesite of the caldera infilling, overlying a small coal seam. Ironically, the highest Ag concentration (62.8 ppm) was found in the coal, not in the mineralized zones in the altered volcanic rocks.

2. SAMPLES

For the work on the ores from Rabenstein and Treiboltz , the same samples as in the previous studies (Majzlan, 2009; Berkh et al., 2014) were used. Some samples of the Schöpfer vein were collected specifically for this work in the accessible portions of the Ján Baptista adit, from its uppermost levels. A precise location of the rich precious metal samples is shown in Fig. 2. The deeper horizons of the adit are inaccessible because they were used for deposition of flotation waste in the second half of 20th century. Additional samples from the Schöpfer vein came from the archive of the Geological Institute of Dionýz Štúr in Bratislava or the Mining museum in Banská Štiavnica. The precise location of these samples is given in Onačila et al. (1993) and Gašparek (2009). Samples from the Bursa vein were collected from two

drillholes, BUVE-1 and BUVE-2 (see point B in Fig. 1), kindly provided for this study by the company EMED Mining. Samples from the Trojkráľová vein are from a surface outcrop and from drillhole A-1a that explored this vein in 1986 (Štohl et al., 1986).

3. METHODS

Samples were prepared as standard thin and polished sections and inspected in transmitted and reflected polarized light. Images were acquired with a Zeiss microscope Axio Imager.M2m and attached digital Zeiss camera AxioCam MRc5 and software Axiovision.

Selected ore sections were analyzed by wave-dispersive spectrometry (WDS) with a Cameca SX100 electron microprobe (National Museum Prague), using these standards and emission lines: Au (Au, Mα), S, Cu ($CuFeS_2$, Kα), Bi (Bi_2Se_3, Mβ), Ag (Ag, Lα), Sb (Sb_2S_3, Lα), Pb (PbS, Mα), Cl (NaCl, Kα), Hg (HgTe, Lα), Fe (FeS_2, Kα), Zn (ZnS, Kα), Ni (Ni, Kα), As (NiAs, Lβ), Se (PbSe, Lβ), Cd (CdTe, Lα), Co (Co, Kα), Mn (Mn, Kα), Sn (Sn, Lα). Au-Ag alloys were analyzed with accelerating voltage of 25 kV and current of 20 nA, sulfides with 25 kV and 10 nA. Beam diameter was 2 μm. Back-scattered electron images were also acquired with this instrument. All electron microprobe analyses of sulfides are listed in supplementary tables S1-S5, deposited electronically with this manuscript.

Table 1. Representative electron microprobe analyses of acanthite, galena, and polybasite/pearceite from the Schöpfer vein. All analyses are listed in the electronic supplementary information. All elements analyzed for which the concentration was always 0.00 wt.% are not listed. For the list of analyzed elements, see the section Methods. Bottom part of the table shows the same analyses recalculated to atomic % for acanthite and galena and based on 29 atoms for polybasite/pearceite.

Sample	mineral	S	Ag	Sb	Pb	Cu	Fe	Zn	As	Total
HDS7	acanthite	12.43	86.14	0.00	0.00	0.18	0.00	0.00	0.33	99.08
HDS3	acanthite	12.10	86.95	0.00	0.00	0.00	0.00	0.16	0.27	99.47
HDS2	acanthite	14.81	84.04	0.00	0.00	0.10	0.00	0.00	0.25	99.20
HDS3	galena	13.94	0.00	0.00	86.56	0.00	0.00	0.00	0.00	100.50
HDS2	polyb/pearc	12.88	74.06	8.43	0.00	3.74	0.08	0.02	0.84	100.06
HDS5	polyb/pearc	15.38	68.82	8.32	0.00	6.00	0.00	0.00	1.37	99.89
HDS5	polyb/pearc	11.45	75.02	5.82	0.00	5.07	0.00	0.00	1.85	99.20
HDS5	polyb/pearc	14.30	70.90	5.15	0.00	5.96	0.00	0.00	2.72	99.03
HDS2	polyb/pearc	15.22	70.15	4.73	0.00	5.48	0.00	0.00	3.65	99.24
HDS2	polyb/pearc	15.19	70.05	4.01	0.00	5.67	0.00	0.00	4.35	99.26
HDS2	polyb/pearc	15.46	70.12	2.75	0.00	6.23	0.00	0.00	5.33	99.88
HDS7	polyb/pearc	14.68	72.36	2.47	0.00	6.24	0.09	0.00	5.12	100.97
HDS2	polyb/pearc	15.50	70.77	1.80	0.00	5.83	0.00	0.00	5.45	99.35
HDS7	polyb/pearc	16.01	70.26	0.81	0.00	7.11	0.00	0.00	6.20	100.39
HDS7	polyb/pearc	15.81	71.47	0.47	0.00	6.80	0.00	0.00	6.37	100.91
HDS3	polyb/pearc	14.59	76.88	0.00	0.00	2.92	0.00	0.00	6.30	100.68

Sample	mineral	S	Ag	Sb	Pb	Cu	Fe	Zn	As
HDS7	acanthite	32.49	66.90	0.00	0.00	0.24	0.00	0.00	0.37
HDS3	acanthite	31.74	67.75	0.00	0.00	0.00	0.00	0.21	0.30
HDS2	acanthite	37.09	62.52	0.00	0.00	0.13	0.00	0.00	0.27
HDS3	galena	51.10	0.00	0.00	48.90	0.00	0.00	0.00	0.00
HDS2	polyb/pearc	9.480	16.194	1.633	0.000	1.388	0.034	0.007	0.264
HDS5	polyb/pearc	10.715	14.244	1.526	0.000	2.108	0.000	0.000	0.408
HDS5	polyb/pearc	8.598	16.737	1.150	0.000	1.920	0.000	0.000	0.594
HDS5	polyb/pearc	10.142	14.939	0.961	0.000	2.132	0.000	0.000	0.825
HDS2	polyb/pearc	10.602	14.518	0.867	0.000	1.925	0.000	0.000	1.088
HDS2	polyb/pearc	10.545	14.446	0.733	0.000	1.985	0.000	0.000	1.292
HDS2	polyb/pearc	10.565	14.236	0.495	0.000	2.147	0.000	0.000	1.558
HDS7	polyb/pearc	10.084	14.767	0.447	0.000	2.162	0.035	0.000	1.504
HDS2	polyb/pearc	10.634	14.424	0.325	0.000	2.017	0.000	0.000	1.599
HDS7	polyb/pearc	10.714	13.969	0.143	0.000	2.400	0.000	0.000	1.775
HDS7	polyb/pearc	10.584	14.214	0.083	0.000	2.296	0.000	0.000	1.824
HDS3	polyb/pearc	10.172	15.923	0.000	0.000	1.027	0.000	0.000	1.879

WDS analyses of carbonates were acquired with a JEOL Superprobe JXA-8230 (University Jena) with these conditions and standards: Fe (Fe_2O_3, Kα), Mg (MgO, Kα), Ca ($CaCO_3$, Kα), Mn (rhodonite, Kα), Ba ($BaSO_4$, Lα), Sr ($SrSO_4$, Lα). Accelerating voltage was 15 kV and current 15 nA. Beam diameter was 5 μm.

For fluid inclusion studies, doubly polished wafers (200-300 μm thick) were studied by a Linkam THM-600 heating–freezing stage. Homogenization temperature was determined upon heating until the inclusion, initially composed of several phases, contained only a single homogeneous fluid. The heating rate was gradually reduced from 20 °C/min to 5 °C/min for an accurate measurement. Eutectic temperatures (Te) were determined during cooling until the liquid phase has frozen, and then observing the first melting during heating of frozen inclusions upon rewarming. Composition of the solutions was estimated by comparing of eutectic temperatures with published data for eutectic temperatures of various salt-water systems (Shepherd et al., 1985 and Bodnar, 2003). The salinity of the fluid was estimated by observing the melting temperature of last ice crystal upon the rewarming. The heating rate was gradually reduced from 10 °C/min to 0.1 °C/min during these measurements. The salinity was then calculated from the freezing-point depression tables by Bodnar (1993). Triple points of natural inclusions of liquid CO_2 (–56.6 °C), distilled water (0 °C), and sulfur (119.2 °C) were used for calibration of the equipment. All microthermometric data and observations are listed in the supplementary table S6, electronically deposited with this manuscript.

Carbon and oxygen isotopes of carbonates were measured using an automated carbonate preparation system Gasbench coupled to isotope ratio mass spectrometer MAT253 (Thermo). Powdered samples of ca. 600–800 mg were flushed with helium in septum-sealed glass vials, then reacted with anhydrous H_3PO_4 for 24 hours at 25 °C. The CO_2 yield is chromatographically separated and introduced into the mass spectrometer in continuous flow mode (helium as carrier gas), whereby three injections of reference gas are followed by four injections of sample aliquots. A set of working standards, traceable to international standards will be regularly scattered between samples to check for accuracy. Usual precision of the method is 0.2 ‰ for $\delta^{18}O$ and 0.1 ‰ for $\delta^{13}C$.

4. RESULTS

4.1 Rabenstein

The mineralized zone at Rabenstein is made of massive or cellular quartz with numerous strongly altered lithoclasts. The cellular quartz is thought to originate by dissolution of earlier carbonates; in our work, we have found no carbonates left in the samples from Rabenstein. The alteration erased essentially all primary features in the lithoclasts and these are mostly seen in thin sections as darker outlines made of fine-grained mixture of minerals. The lithoclasts are cemented by fine-grained quartz whose grain size increases into the space between the fragments. Thin veinlets of younger quartz crosscut the entire hydrothermal breccia. This younger quartz is coarser and forms often druses in the center of the veinlets. It is also probable that the ubiquitous druses of minute quartz crystals in the voids of the cellular quartz belong to this late quartz generation.

Table 2. Isotopic composition of calcite samples from the Schöpfer vein. All data in ‰.

sample	$\delta^{13}C$	$\delta^{18}O_{VSMOW}$	$\delta^{18}O_{fluidVSMOW*}$
calcite, coarse, older	–4.58	4.20	–4.34
calcite, coarse, younger	–4.81	3.99	–4.55
calcite, scalenohedra	–0.98	10.65	
calcite, scalenohedra	–1.27	10.14	

*calculated for T = 220 °C with the fractionation factor from Friedman & O'Neil (1977)

The ore mineralogy of Rabenstein was investigated by Onačila et al. (1993) and Majzlan (2009) who reported abundant pyrite, galena, sphalerite, and infrequent chalcopyrite and marcasite. Precious-metal minerals are represented by acanthite, freibergite, electrum, polybasite-pearceite, pyrargyrite, and late uytenbogaardtite and acanthite. Ore minerals are found in the strongly altered lithoclasts or in the fine-grained quartz that cements, replaces, and penetrates the lithoclasts. The young drusy quartz contains no ore minerals.

The massive quartz samples from Rabenstein contain mostly fine-grained quartz devoid of fluid inclusions. Even some of the larger quartz crystals contain no inclusions. In this work, we screened several samples but could measure only one (Rab10) where the fluid inclusions were hosted by larger, subhedral quartz crystals that belong to the youngest, barren generation of quartz. Most of the inclusions measured were recognized as primary according to the criteria of Roedder (1984). They contain aqueous and gas phase in variable proportions, suggesting boiling of the fluid at the time of inclusion. Only liquid-dominated fluid inclusions were measured. The salinity of the measured fluids varies between 2.9 and 4.8 wt.% NaCl eq. and homogenization temperature between 223 and 270 °C (Fig. 3). Reliable eutectic temperatures could not have been measured; a few observations indicate that they may lie between –35 and –25 °C. Three inclusions that were identified as secondary gave similar salinities and homogenization temperatures of 156, 261, and 265 °C.

4.2 Treiboltz

The samples from Treiboltz consist of hydrothermal breccias with two generations of quartz. The lithoclasts are made of porous country rocks (perhaps tuffs) whose pores were cemented by the first, fine-grained generation of quartz. In addition, this quartz penetrates the clasts, replaces them, and builds the matrix between the lithoclasts. This matrix-supported breccia is penetrated by numerous veinlets of younger, coarse-grained quartz.

The ore minerals at Treiboltz are dominated by pyrite, galena, and sphalerite (Berkh et al. 2014). Chalcopyrite is infrequent. Minerals of precious metals include hessite, benleonardite, and rare tellurosulfides. There are also trace amounts of freibergite, polybasite-pearceite, and acanthite. The abundance of tellurium in these ores distinguishes this locality from many others in the Hodruša-Hámre ore district. The ore minerals are restricted to the altered lithoclasts and the older, fine-grained quartz.

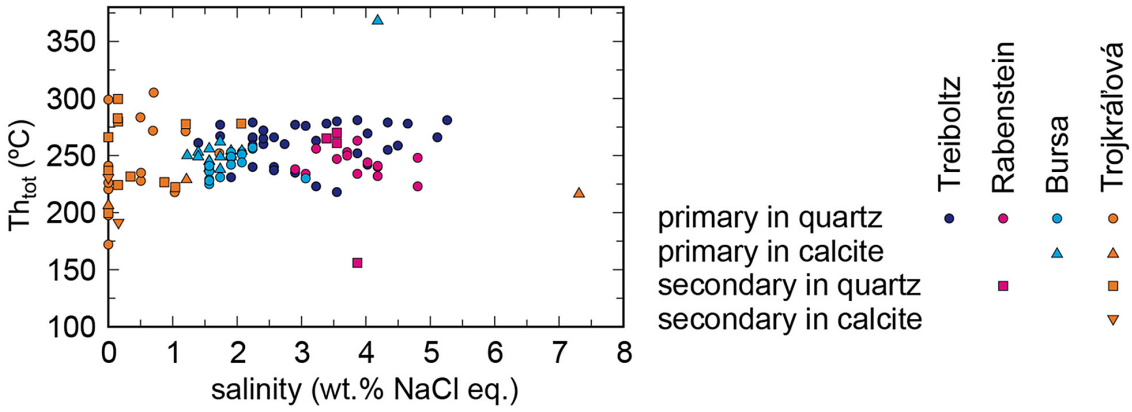

Fig. 3. Salinities and total homogenization temperatures for fluid inclusions from Treiboltz, Rabenstein, Trojkráľová, and Bursa.

The older, fine-grained quartz contains no inclusions. The fluid inclusions measured in this work were found in several samples in the younger, coarse-crystalline quartz (Figs. 3, 4). As in Rabenstein, the inclusions contain two phases, liquid and gas, in variable proportions, indicating boiling. All inclusions measured were primary, dominated by the liquid (aqueous) phase, with salinities between 1.4 and 5.3 wt.% NaCl eq. and homogenization temperatures of 218 to 281 °C (Fig. 3).

4.3 Bursa

As at the other localities, the ore body consists of hydrothermal breccia with strong alteration. The altered andesite fragments show extensive adularization. Rarely, acicular crystals of epidote were seen in the optical microscope. Fine-grained sheet silicates, abundant in the samples, were identified as illite, with negligible proportion of expandable layers. The space between

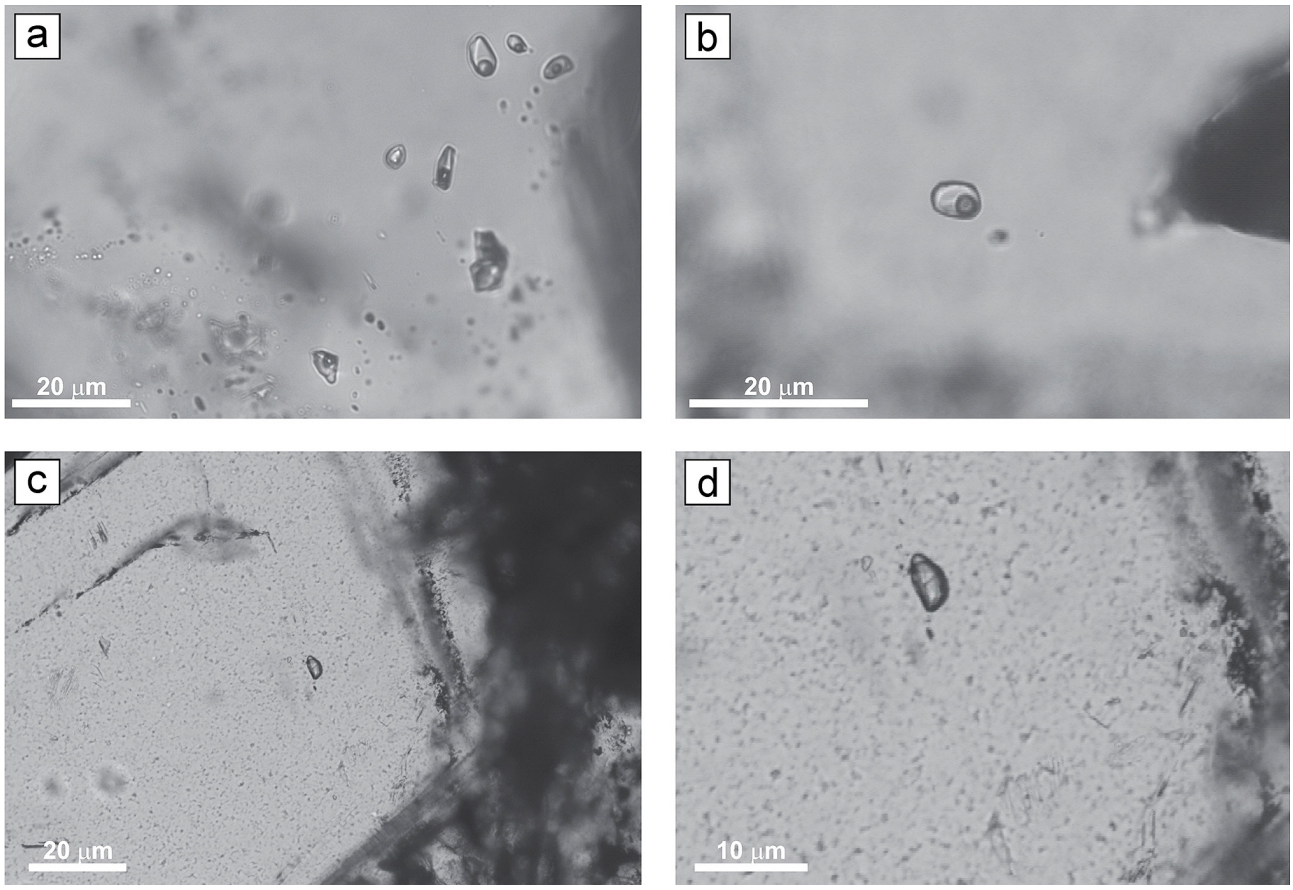

Fig. 4. Images of fluid inclusions in the samples studied, taken in transmitted polarized light. a) A group of L+V inclusions in quartz from Treiboltz. b) L+V inclusion in quartz from Schöpfer, dominated by aqueous phase. c,d) L+V inclusion in quartz from Schöpfer, dominated by gas phase. The image d) is a detail of c). Small amount of aqueous phase is visible in the upper tip of the inclusion.

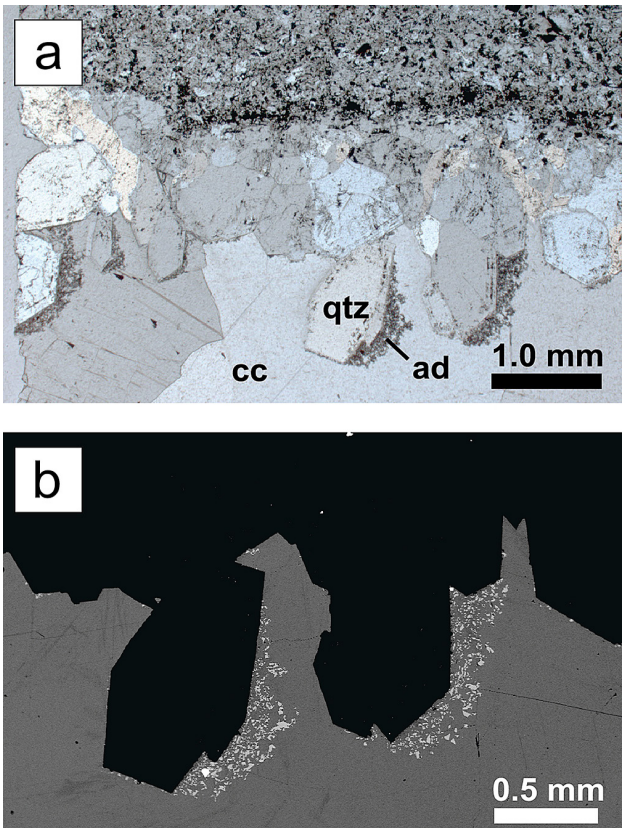

Fig. 5. Images of gangue and ore minerals from Bursa. a) optical image in transmitted polarized light, crossed nicols, of an altered lithoclast (upper portion of the photograph), overgrown by euhedral quartz (qtz) crystals. The quartz crystals are coated by porous aggregates of fine-grained adularia (ad) from one side. The space between the lithoclasts is filled by coarse calcite (cc). b) BSE image of a detail of a). Quartz appears here as black, calcite is grey, adularia light grey. The small white grain is pyrite.

the altered lithoclasts is filled by druses of euhedral quartz crystals, with sprinkling of adularia (Fig. 5). The final stage of mineralization was filling of the druses and open spaces with coarse-grained calcite.

Ore minerals in the drillhole samples from Bursa are relatively infrequent. Pyrite dominates, either in the altered lithoclasts or in the gangue minerals (quartz, calcite). Sphalerite, chalcopyrite, and galena are also present, but in lesser amounts. Such mineralization was detected in depth of 129-131 meters in the drillhole BUVE-2, characterized by intergrowths of the base-metal minerals and chemically heterogeneous, As-enriched pyrite (Fig. 6). This section of the drillhole has also the highest Au concentration (0.21-0.29 ppm). In the drillhole BUVE-1 (8.8 m), only weak pyrite mineralization was found in the depth of 8.8 m. No minerals of precious metals were found in either sample available from the drilling program.

Fluid inclusions were found in the hydrothermal quartz and calcite. All measured inclusions were identified as primary. They form a tight cluster (Fig. 3) with two outliers. Within the cluster, the salinities vary between 1.2 and 2.2 wt.% NaCl eq. and homogenization temperatures between 225 and 262 °C. The two outliers have higher salinity (3.0 and 4.2 wt.% NaCl eq.) and homogenization temperatures of 230 and 368 °C, respectively. The average homogenization temperature for the inclusions in calcite (BUVE-1, 8.8 m: 250 °C) is somewhat higher than the homogenization temperature in quartz (sample BUVE-2, 122.1 m: 233 °C; BUVE-2, 124.2 m: 247 °C).

4.4 Trojkráľová

Trojkráľová vein was studied from a surface sample and from the drillhole A-1a. The surface sample was a coarse-grained calcite with cavities filled by tiny transparent quartz crystals. The drillhole sample comes from depth 233.2 and 270.2 m, representing 45 m long section of the hole with silicified carbonate rocks – brecciated grey dolomite partially metasomatically altered to talc and penetrated by irregular network of quartz and carbonate veinlets (Onačila & Rojkovičová, 1989). Fine-grained pyrite is abundant in tectonic breccias in the depth of 278.0 meters. The analysis of the drillhole section 203.4 – 204.2 meters gave 2.2 g/t Au and 13 g/t Ag (Lexa et al., 1997).

Vein carbonates in the studied samples belong to calcite or Mn-calcite (A-1a/270.2), rarely to dolomite (A-1a/233.2).

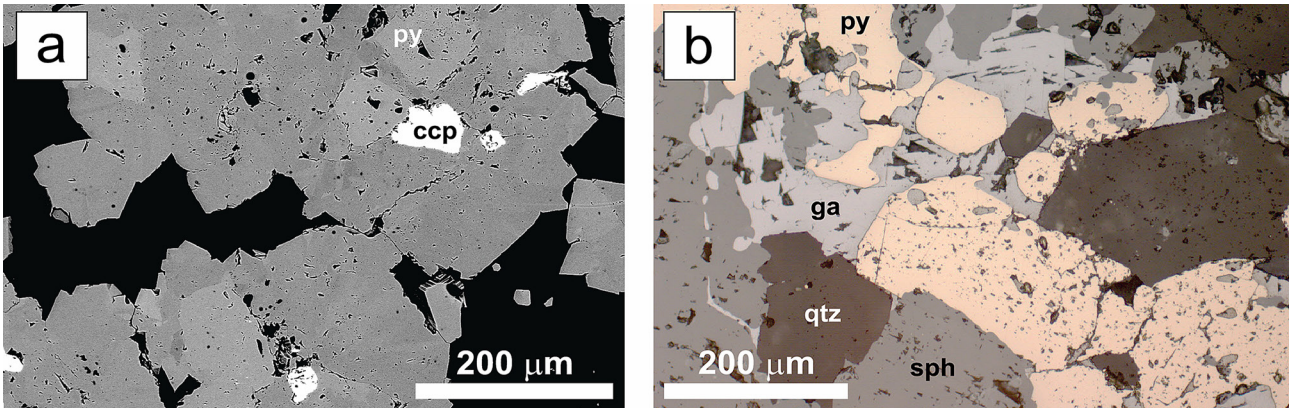

Fig. 6. Images of ore minerals from Bursa. a) BSE image of heterogeneous pyrite of patches with different composition (py, different As concentration, shades of grey) and small chalcopyrite grains (ccp, white) in the center of the aggregates (drillhole BUVE–2, depth 122.1 m); b) optical image in polarized reflected light, showing galena (ga, white), pyrite (py, yellowish), sphalerite (sph, light grey), and quartz (qtz, darker grey) (drillhole BUVE–2, depth 130.0 m).

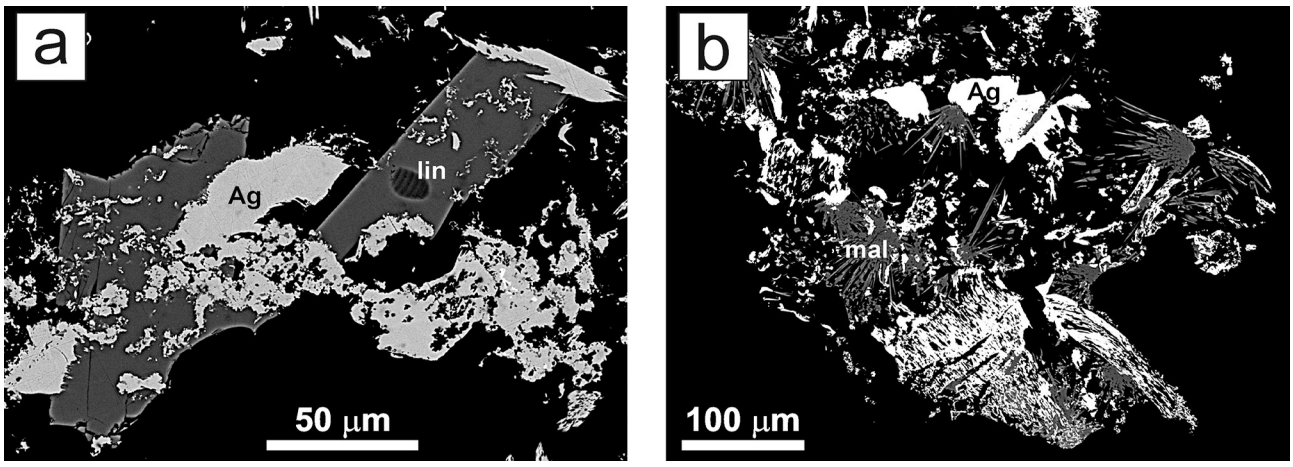

Fig. 7. Back-scattered electron (BSE) images of secondary minerals from the Schöpfer vein. a) linarite (lin, darker grey) and silver (Ag, light grey); b) malachite (mal, dark grey, radial) and silver (Ag, white).

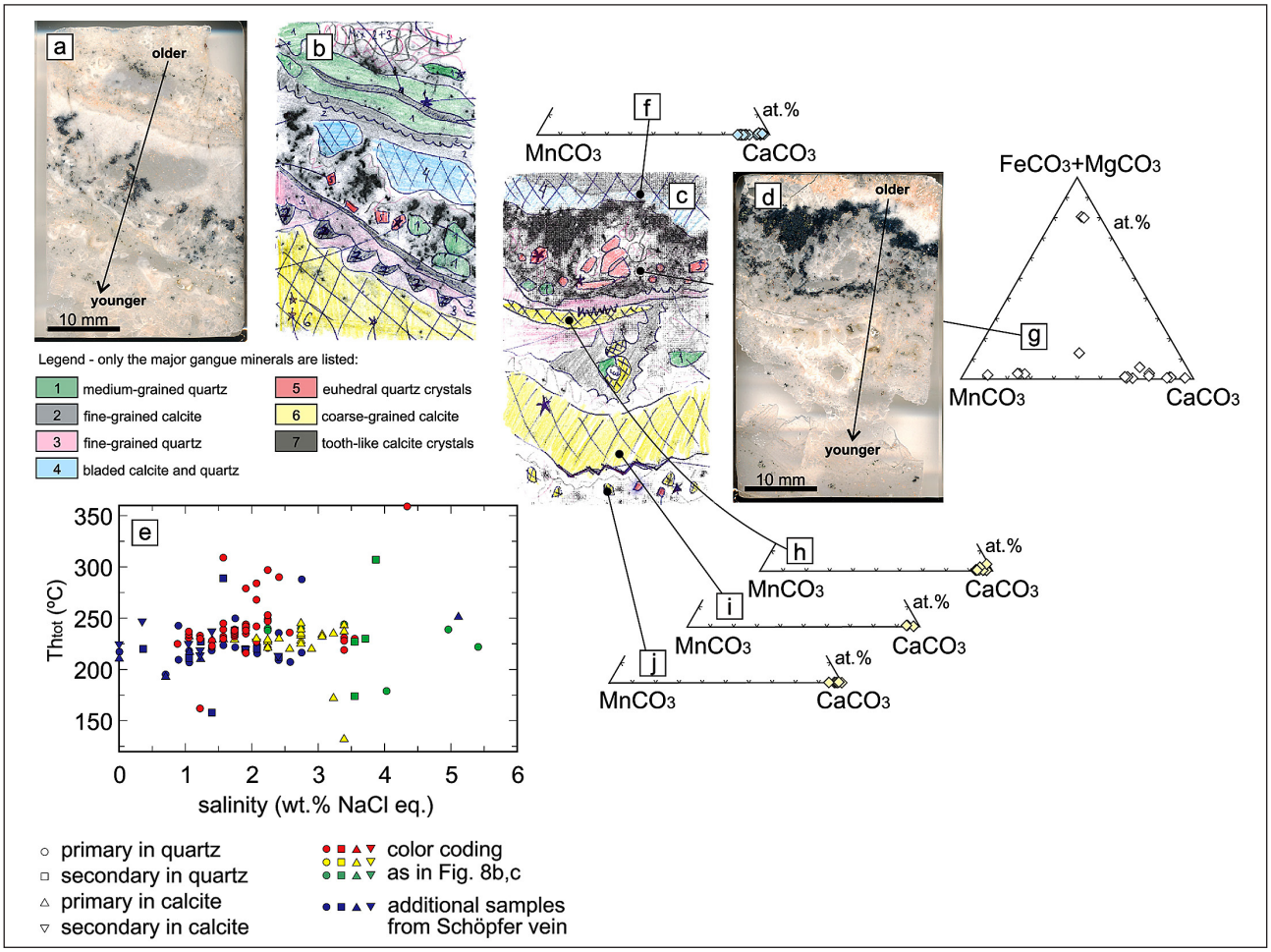

Fig. 8. Overview of textures of the hydrothermal samples, measurements on fluid inclusions, and chemical composition of carbonates from the samples from Schöpfer. a,d) photographs of double-side polished thick sections; b,c) corresponding documentation after petrographic investigation of the sections in a,d. Color coding is used to show the major gangue minerals. Detailed description is in the text and microscopic images in Fig. 9. Ore minerals are not color coded; they appear in a-d as black patches. Note that these two samples were not taken next to each other. They are only positioned in this figure so that the correlation between their individual portions is easier to see. The hand-drawn stars in a,d) served for the documentation of the fluid inclusions and can be neglected here. e) Total homogenization temperature and salinity of the fluid inclusions from the samples from Schöpfer. Colors of the symbols (yellow, red, green) correspond to the color coding in the documentation of the sections (b,c). Blue symbols represent measurements in additional samples from the Schöpfer vein (see text). f-j) Chemical composition of carbonates from different parts of the samples. All data are from electron microprobe analyses. Black circles show the portions of the sections where the analyses were acquired. These are, however, not the exact analytical spots.

Other ore or gangue minerals were not studied in a detail.

Most of the studied fluid inclusions were located in quartz, fewer in calcite. Salinities (Fig. 3) are low, less than 3 wt.% NaCl with a single exception of 7.3 wt.% NaCl. Homogenization temperatures varied between 169-303 °C, with average temperatures between 219-260 °C. The variable liquid/gas ratio in the inclusions, however, indicates trapping of a heterogeneous fluid, probably in the state of boiling. Therefore, the true trapping temperatures should be the lowest recorded temperatures for each population of fluid inclusions. We estimated this temperature to about 220 °C for both studied samples.

4.5 Schöpfer

Several types of samples were collected from the old accessible portions of the adit which opened significant portions of the Schöpfer vein. One set of samples, collected from the upper parts of Luiza stope and other abandoned stopes located above the first level, contained secondary minerals and sparse relics of the primary mineralization. The secondary minerals include cerussite, todorokite, silver, malachite-rosasite, smithsonite and linarite (Fig. 7).

Another set of samples were those collected during mining, prior to year 1950, or during field campaigns of scientific staff of the Geological Institute of Dionýz Štúr in Bratislava. These samples consist mostly of calcite and quartz with weak sulfide mineralization. Calcite is almost pure $CaCO_3$ with a minor $MnCO_3$ component. Fluid inclusions with sizes up to 150 μm were found both in quartz and calcite. The few measured values of eutectic temperatures varied between –25 and –34 °C and indicate NaCl as the major electrolyte, perhaps with additional $FeCl_2$ or $MgCl_2$. Salinities and total homogenization temperatures are shown by blue symbols in Fig. 8e. Salinities are low, less than 3 wt.% NaCl eq. with a single exception of 5.1 wt.% NaCl eq. Homogenization temperatures varied between 195-287 °C (mean temperatures for individual samples in the range 211-231 °C) for the primary inclusions and 157-287°C (mean in range 216-225°C) for the secondary inclusions.

The last sample set originated from the Luiza stope, which is located between the first and second level of the Schöpfer mine (shown in Fig. 2 by red dots). The studied samples show perplexing complexity on the microscopic scale. On the scale of a thin section, a number of different styles of precipitation, in terms of their mineralogical content and ore textures, can be recognized (Figs. 8 and 9). Microscopic observations clearly document that the minerals grew into open space and allow to establish relative timing of the precipitation in our sections (shown by black arrows in Fig. 8a,d). The gangue minerals detected are quartz of variable grain size, adularia, and different carbonates.

Precipitation of sulfides was preceded by formation of bladed calcite, chemically almost pure $CaCO_3$, with a minor $MnCO_3$ component (Fig. 8f). This calcite is replaced to a variable degree by quartz (Fig. 9b-d). Calcite is porous, inhomogeneous, with patches of variable composition (Fig. 9d). It is not clear if the replacement of calcite by quartz occurred before the deposition of the sulfides, together with them or later. In some cases, the bladed calcite crystals enclosed in the mass of quartz, in other cases, the aggregate is mostly made of calcite, with incipient replacement by quartz (Fig. 9b-d).

The following event was the deposition of sulfides (Fig. 9e,f). Base-metal minerals include pyrite, chalcopyrite, sphalerite, and galena. Of those, sphalerite predominates over the other ones. The base-metal sulfides are accompanied by abundant members of the polybasite-pearceite solid solution, acanthite, and electrum (Fig. 10). Minor amounts of stephanite and pyrargyrite were also observed. The minerals of Ag and Au are coeval (Figs. 9e,10a-c) or later (Fig. 10d) than the base-metal sulfides. The polybasite-pearceite solid solution spans almost the entire range between the Sb (polybasite) and As (pearceite) end-members, with the exception of pure Sb compositions (Fig. 11, Tab. 1). Acanthite corresponds well to the nominal composition Ag_2S, with slightly elevated Cu (up to 0.24 at.%) and As (0.63 at.%) content. Galena is pure PbS, with Bi, Au, Sb, Sn, Cu, Fe, Zn, Ni, Hg, Co, As, Se, Cd, Mn concentration being 0.00 wt. % in all analyses. Only one analysis gave 0.12 at. % Ag, all other ones 0.00 wt. %. The electrum grains have uniformly low fineness, with 50 wt. % Au and 50 wt. % Ag (36 at. % Au and 64 at. % Ag). All other elements in electrum were below the detection limit except for Zn, with the highest concentration measured of 1.67 at. %.

The richest sulfide aggregates are intergrown with quartz. In such aggregates (example shown in Fig. 9e,f), sulfides are more abundant than quartz. As the precipitation of sulfides was waning, the fluids also deposited carbonates and adularia (Fig. 9g,h). Spatial association of carbonates and sulfides (Fig. 9g) suggests a genetic link between the two groups of minerals in this process. The composition of carbonates is rather variable (Fig. 8g). In addition to calcite with minor $MnCO_3$, we found also small inclusions of rhodochrosite (Fig. 9g), siderite (Fig. 9h), and kutnahorite. EDS analyses identified also tiny grains of carbonates dominated by Zn, perhaps smithsonite.

In the ore-bearing zone, fluid inclusions (Fig. 4b-d) were found only in euhedral quartz crystals (marked red in Fig. 8b,c, see also Fig. 9i) or medium-grained quartz (marked green in Fig. 8b,c). Quartz in the richest sulfide aggregates is fine-grained and contains no fluid inclusions. Inclusions in the euhedral quartz crystals are mostly of low salinity (< 2.5 wt. % NaCl eq.) (Fig. 8e). Apart from one outlier, the homogenization temperatures are higher than 216 °C. The inclusions showed signs of boiling and heterogeneous trapping, so that temperatures of ~220 °C could be assumed as trapping temperatures. Beside fluid inclusions, these quartz crystals contain also tiny, perfectly euhedral calcite inclusions (Fig. 9j) (calcite identified by Raman spectroscopy). The data for the fluid inclusions in the medium-grained quartz are more scattered, but generally with higher salinity (3.5-5.4 wt.% NaCl eq.) (Fig. 8e). Of the four measured inclusions associated with the ores, two show Th_{tot} of ~230 °C, one 174 °C and the last one 307 °C. Given the small number of observations, it is difficult to explain these variations. It is also not clear which population of the inclusions, if any (from the euhedral or medium-grained quartz) could be genetically linked to the sulfide-precipitating fluid.

Once the precipitation of sulfides and accompanying gangue minerals ceased, barren carbonates (Figs. 8c) with near-calcite composition (Fig. 8h) were formed. They were followed by quartz

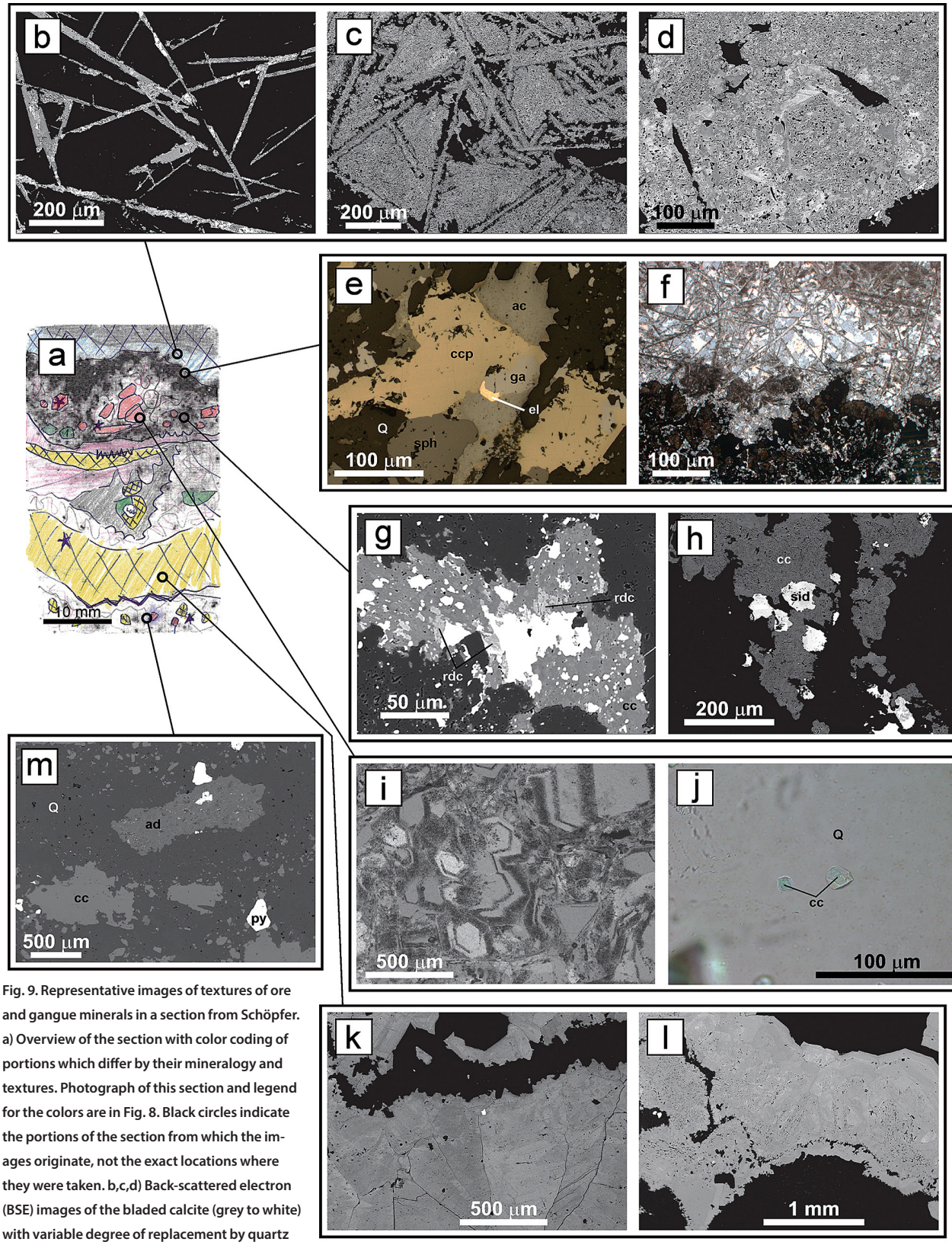

Fig. 9. Representative images of textures of ore and gangue minerals in a section from Schöpfer. a) Overview of the section with color coding of portions which differ by their mineralogy and textures. Photograph of this section and legend for the colors are in Fig. 8. Black circles indicate the portions of the section from which the images originate, not the exact locations where they were taken. b,c,d) Back-scattered electron (BSE) images of the bladed calcite (grey to white) with variable degree of replacement by quartz (black). The image d) shows the porosity and inhomogeneity of this calcite. e) Rich ore aggregate with common sphalerite (sph), chalcopyrite (ccp), and galena (ga). Minerals of precious metals are acanthite (ac) and electrum (el). Reflected light. f) Transition of the bladed calcite with quartz to an ore aggregate dominated by sphalerite. Transmitted light. g) An aggregate of carbonates (calcite - cc, rhodochrosite - rdc) associated with ore minerals (undifferentiated, white) in quartz (black). BSE image. h) An intergrowth of calcite (cc) and siderite (sid) in quartz (black). BSE image. I) Euhedral quartz crystals. Transmitted light. j) Euhedral calcite inclusions in the euhedral quartz crystals. Transmitted light. k,l) Coarse-grained calcite with patches of slightly variable composition (different shades of grey) with crystals of pyrite (white) in quartz (black). BSE images. m) A mixture of quartz (Q), adularia (ad), calcite (cc), and pyrite (py). BSE image.

of different grain sizes, intergrown with carbonates. Afterwards, another precipitation of carbonates took place. Tooth-like aggregates of calcite were visible in one sample (dark grey in Fig. 8b), but all samples showed the presence of coarse-grained, barren calcite (yellow in Fig. 8b,c) with sparse pyrite crystals (Figs. 8i, 9k,l). Primary fluid inclusions in this coarse calcite have salinities between 1.7-3.4 wt.% NaCl eq. and homogenization temperatures of 220-245 °C, with two outliers that are lower (Fig. 8e). The last zone captured in our sections is made of a mixture of quartz, large anhedral calcite grains (Fig. 8j) and adularia, with some pyrite (Fig. 9m).

The isotopic composition of calcite in our samples from Schöpfer is listed in Tab. 2. We separated the coarse calcite with the fluid inclusions measured (details in the previous paragraph) and scalenohedral calcite crystals in small fissures in the coarse calcite. The coarse calcite marked as "older" and "younger" originated from the same samples presented in detail above. The precipitation sequence, determined on our samples, is marked by arrows in Fig. 8a,d. Assuming the precipitation temperature of 220 °C (determined from the homogenization temperatures of fluid inclusions), the $\delta^{18}O_{fluid}$ is –4.34 and –4.55 ‰. These values are isotopically lighter as those reported for the older Au mineralization at the deep levels of the Rozália mine (–2.7 to +1.1‰, Koděra et al., 2014), suggesting an increasing proportion of meteoric fluids in the hydrothermal system for the late epithermal Ag-Au mineralization. The scalenohedral crystals on the fractures of the coarse calcite are isotopically heavier. Their formation temperature, however, is not known, and the heavier signature may be the result of crystallization at lower temperatures. If we speculate that they formed from pure meteoric water (Sarmatian meteoric water at the geographic position of the today's region of Banská Štiavnica, isotopic composition estimated by Koděra et al. 2005), then their crystallization temperature (in isotopic equilibrium) should have been about 70 °C. A very late, low-temperature overprint was documented at a number of localities in Hodruša-Hámre and vicinity by the replacement of electrum by the low-temperature phase uytenbogaardite (Majzlan, 2009; Berkh et al., 2014). Therefore, such interpretation is likely, although not supported here by other data.

5. DISCUSSION

The samples and localities studied within this work show a variety from simple hydrothermal breccias to large and complex epithermal veins. Treiboltz, Bursa, and partially Rabenstein belong to the first category. Hydrothermal breccias are cemented by ore-bearing quartz, later penetrated by younger quartz (Treiboltz, Rabenstein) or sealed by calcite (Bursa). At Treiboltz and Rabenstein, no fluid inclusions were found in quartz that hosts the ore minerals. This quartz is fine-grained and could be perhaps interpreted as a recrystallization product from a cryptocrystalline SiO_2 variety such as chalcedony, which means formation temperatures of <200 °C. At temperatures above 200 °C, hydrothermal fluids should precipitate only the stable SiO_2 phase, that is, quartz, and not the metastable ones (Dove & Rimstidt, 1994). Fluid inclusions from the younger, barren quartz, however, indicate trapping temperatures between 200-250 °C (Fig. 3), thus challenging the hypothesis of recrystallization of the older quartz from chalcedony. Dong et al. (1995), however, argue that boiling and cooling of a fluid to ~220 °C could cause not only precipitation of quartz but also of amorphous silica. They consider the presence of the quartz textures inherited from silica gel, in addition to fluid inclusion or other evidence to be a good indicator of boiling in epithermal environments. Bodnar et al. (1985) report, on the other hand, the possibility that the variable liquid/gas ratio in some samples could be caused by maturation of fluid inclusions, not by trapping of heterogeneous fluid. In our case, however, there are other indicators (other than the fluid inclusions alone) that point out at boiling of the fluids, and we prefer to explain the variable phase ratios in the inclusions in the studied samples by boiling.

Assuming boiling fluids and hydrostatic pressure conditions, the depth of deposition of the gangue and ore minerals could be estimated to ~250 meters. This datum relates to the temperature of 220 °C and dilute aqueous fluid, as the one enclosed in the fluid inclusions studied here.

At Rabenstein, the mineralized zone contains massive blocks of porous, "cellular" quartz. This type of quartz is traditionally interpreted as a result of replacement of older bladed carbonate by quartz and dissolution of the carbonates due to continous boiling of fluids (e.g., Koděra et al., 2007). Hence, the earlier hydrothermal activity produced here large blocks of bladed carbonates that were completely obliterated by later events. Diminished abundance of carbonates or their absence in the eastern portion of the Hodruša-Hámre ore field (where the Rabenstein occurrence belongs) was already mentioned by Koděra ed. (1986).

Our few samples from the Schöpfer vein certainly cannot describe the entire variability of this ore body but pose some interesting questions. Earlier studies of the Schöpfer vein described quartz-carbonate ores with disseminated pyrite, sphalerite, and chalcopyrite; galena was more abundant in the deeper portions of the vein (Harazim, 1955; Zrůstek, 1957). They reported that the minerals of the precious metals have been mined out and cannot be found anymore. Onačila et al. (1993), however, described electrum, polybasite, pyrargyrite, pyrostilpnite, stephanite, and acanthite in the samples collected underground in the early 1990's, augmented by historical samples from archives. Koděra ed. (1986 and references therein) performed a detailed paragenetic study of the veins in the Hodruša ore field mostly on the Schöpfer and Všechsvätých veins. He distinguished 9 precipitation periods, dominated either by quartz or by carbonates. Only the fifth period should contain minor pyrite, sphalerite, chalcopyrite, and galena, hosted by quartz. He reported that most of the minerals of Ag are secondary; only a small fraction of the Ag minerals are primary, disseminated in carbonate or quartz with base-metal sulfides. Onačila et al. (1993) saw no reasons to distinguish the last 3 periods as separate precipitation events. Onačila & Rojkovičová (1992) simplified the paragenetic scheme by the definition of two ore-forming stages that correspond to the second and fifth period of Koděra ed. (1986). The first stage contains base-metal sulfides, electrum and rare Ag sulfides. The second stage is richer in silver, forming rich accumulations of primary sulfides and sulfosalts of Ag. The abundance of silver

minerals in our samples could assign this mineralization to the second stage of Onačila & Rojkovičová (1992). Some of the silver sulfides are clearly younger than the base-metal sulfides (Fig. 10d).

The most interesting aspect, in our opinion, is the chemical variability of the carbonates associated with the ore minerals Schöpfer vein (Fig. 8g), in strong contrast to the monotonous composition of the barren carbonates (Fig. 8h-j). We identified calcite, rhodochrosite, kutnahorite, siderite, and smithsonite among the carbonates spatially associated with the rich sulfide accumulations. The presence of siderite and smithsonite suggests that the fluids exhausted their capacity to precipitate sulfides by depletion in reduced sulfur, not necessarily in metals. In the simultaneous presence of zinc and reduced sulfur, sphalerite should form readily and rapidly. The same conclusion is indicated by the presence of siderite; in the presence of reduced sulfur, the fluid would have precipitated pyrite, not a carbonate. In comparison with other carbonate portions of the studied samples, the ore-forming fluids had also much more Mn, in order to form rhodochrosite and kutnahorite.

It seems, therefore, that the fluids responsible for the precipitation of the barren carbonates were not hindered in the precipitation of the sulfides by physical or chemical factors. Instead, they simple did not possess the metals necessary to produce sulfides. If they did, the metal load would be probably reflected also in variable composition of the carbonates. Hence, it seems that the ore-forming fluids had a different source than the fluids responsible for the barren quartz or carbonates. In agreement with Koděra et al. (2007), we can speculate about a stronger magmatic contribution in the ore-forming fluids. A tentative piece of evidence for this speculation is the elevated salinity of the fluids in the medium-grained quartz associated with the ores (Fig. 8e). The fluids in the euhedral quartz crystals embedded in the ore zone, however, have much lower salinity (red in Fig. 8e). Koděra et al. (2007) reported that the inclusions in sphalerite from the Všechsvätých vein have a higher salinity than the inclusions in the nearby quartz, thereby also supporting the idea of an influx of magmatic fluids for the ore-forming events.

Koděra et al. (2007) brought also new isotopic data for a number of veins in the Hodruša-Hámre ore field and concluded that the vein quartz is isotopically quite homogeneous. They reported that most of the available $\delta^{18}O$ data for quartz (from their and earlier work) lie in the range of 7.0±1.5 ‰.

A comparison of the salinities of the marginal Trojkráľová vein and the central veins (Figs. 3 and 8e) shows that the inclusions in the marginal vein have the lowest salinities. This observation corresponds well to the low sulfidation nature of the marginal veins when compared to the central ones.

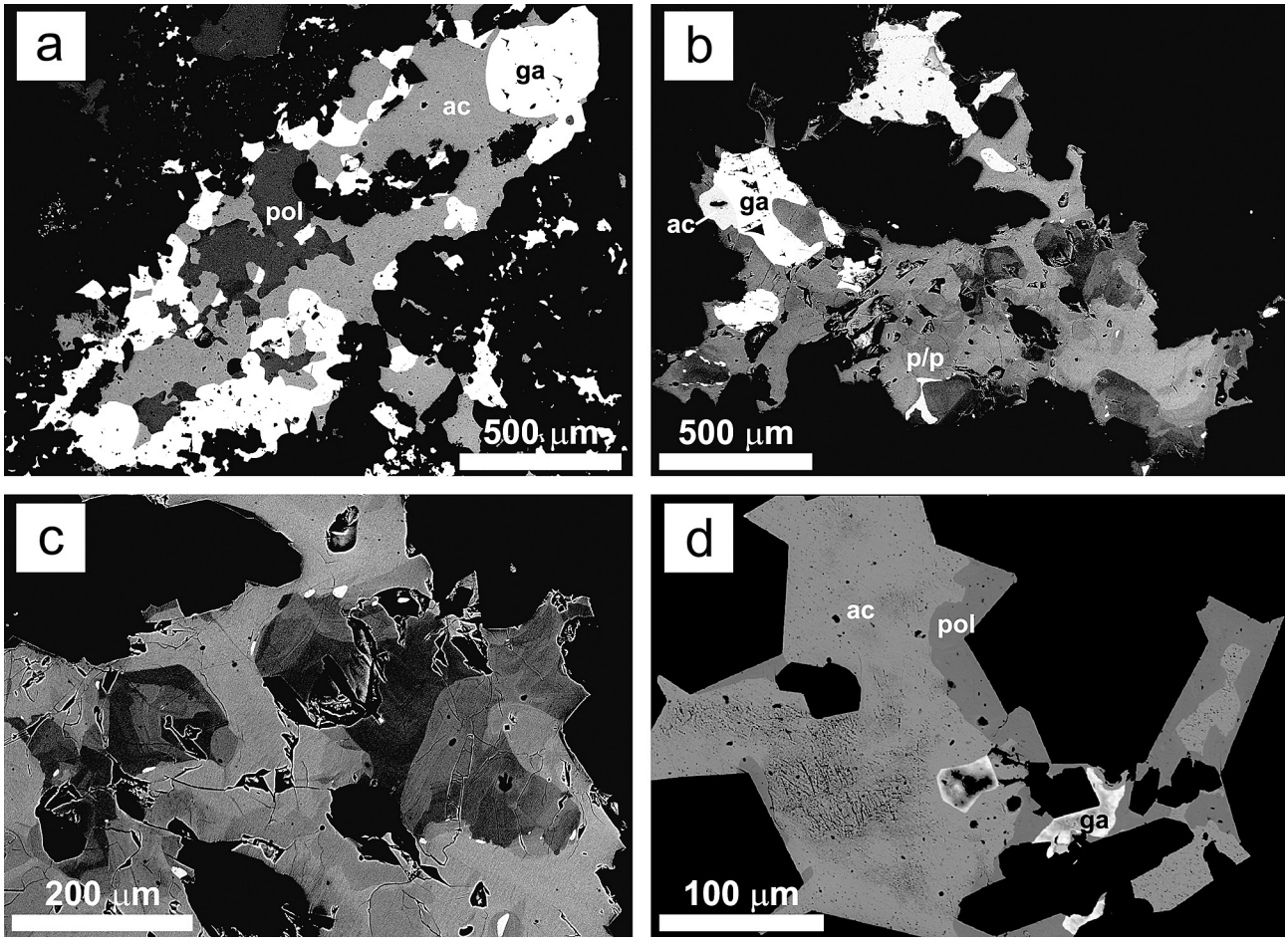

Fig. 10. Back-scattered electron (BSE) images of ore minerals from the Schöpfer vein. a) galena (ga) with acanthite (ac) and polybasite (pol); b) galena with acanthite and zonal polybasite/pearceite (p/p); c) zonal polybasite/pearceite; d) galena relics replaced by acanthite and polybasite.

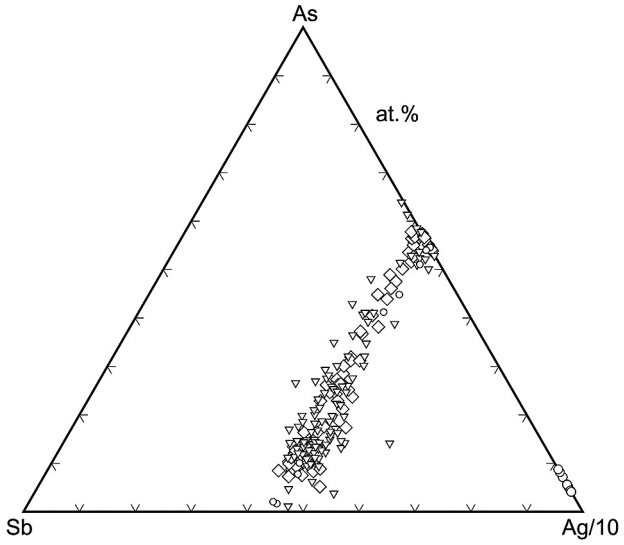

Fig. 11. Chemical composition of polybasite-pearceite and acanthite from the Schöpfer vein in an As-Sb-Ag diagram. The analytical data from the Schöpfer vein (polybasite-pearceite: diamonds, acanthite: circles) are compared to data from Nová Baňa (inverted triangles, Majzlan et al., unpublished data) and Rabenstein (small circles, Majzlan 2009).

A comparison of the fluid inclusion data from this study with previous results is shown in Fig. 12. The fluids of the caldera-collapse related Au mineralization, currently mined in the deep parts of the Rozália mine (Koděra et al., 2014), were hotter than the fluids from the samples studied here. The fluids in the epithermal deposit Nová Baňa (Majzlan et al., unpublished data), in the mantle of the stratovolcano, were somewhat colder. The data for the sulfide-rich veins in Štiavnica ore field (Kovalenker et al., 2006) scatter and overlap with the other data sets. A few inclusions from the Rozália mine and Nová Baňa show much higher salinity than most of the other inclusions. This deviation is explained by "boiling to dryness", excessive boiling that left behind a highly saline fluid. The bulk of the fluid, however, must have been composed of heated dilute waters, probably of meteoric origin.

A comparison of fluid inclusion data for Všechsvätých and Schöpfer Ag-rich veins (Fig. 13), two prominent vein systems in the Hodruša-Hámre ore field, shows that the data clouds are overlapping. The homogenization temperatures for inclusions in quartz and sphalerite from the fifth period from the Všechsvätých vein are lower than the data for the fluids possibly associated with precipitation of sulfides in Schöpfer. The youngest quartz generation studied from the Všechsvätých vein contains inclusions with low salinity (< 1 wt.% NaCl eq.) but the homogenization temperatures remain high. This observation may indicate increasing proportion of meteoric fluids with time but a steady heat supply from the subvolcanic magma chamber. A comparison with data from the Ag-rich veins Rummel-Hoffer (Banky) and Ján Benedikty (Vyhne) (Fig. 14) shows significantly higher temperatures than those measured in the samples from the Schöpfer vein (Onačila et al., 1995). Some of the high homogenization temperatures yield false trapping temperatures, caused by trapping of heterogeneous fluids. Even if entire fluid inclusion populations are taken and the lowest homogenization temperatures considered as the true trapping temperatures, the fluid inclusions from the veins Rummel-Hoffer and Ján Benedikty record hotter conditions than those from Schöpfer. Koděra et al. (2007) argue that the veins Rummel-Hoffer which occur on the boundary between Ag-rich and sulfide-rich veins probably contain both type of veins. The sulfide rich veins in the Štiavnica ore field experienced in general higher fluid temperatures than the Ag-rich veins in the Hodruša ore field.

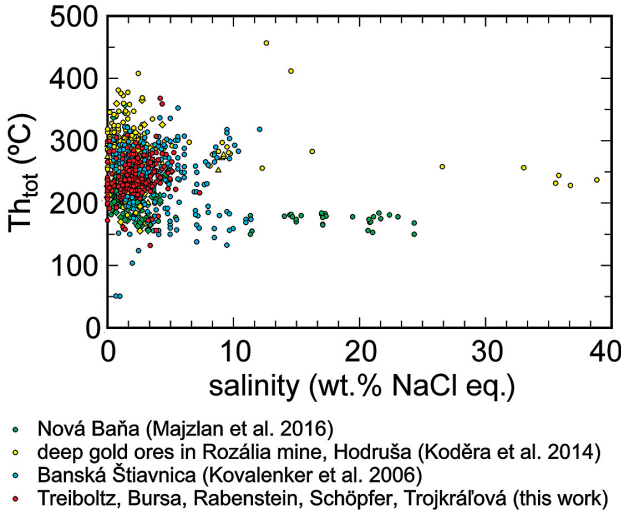

Fig. 12. A comparison of salinities and total homogenization temperatures for fluid inclusions from the sites studied in this work and other epithermal mineralization types in the Banská Štiavnica-Hodruša ore district.

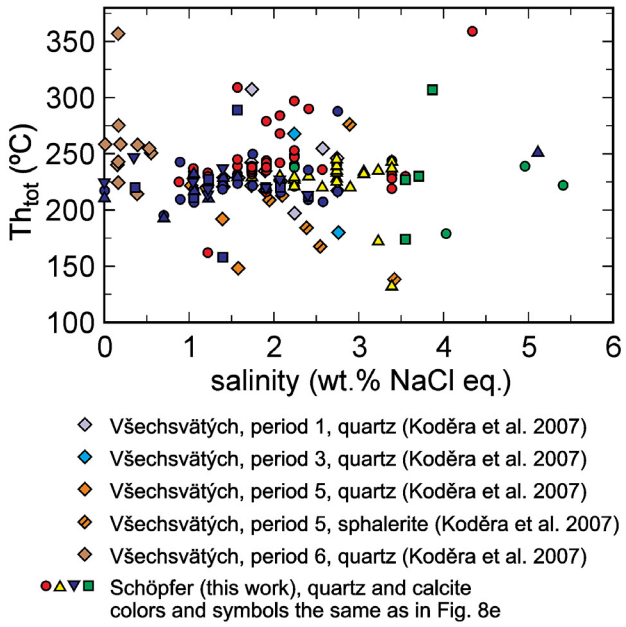

Fig. 13. A comparison of salinities and total homogenization temperatures for fluid inclusions from the Schöpfer vein and different periods (distinguished according to Koděra ed. 1986) of the Všechsvätých vein (data from Koděra et al. 2007, their fig. 44). Only data for primary inclusions from Koděra et al. (2007) are shown.

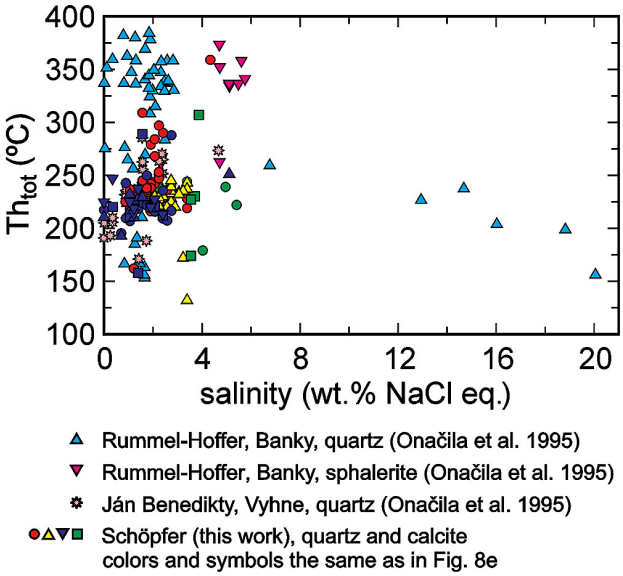

Fig. 14. A comparison of salinities and total homogenization temperatures for fluid inclusions from the Schöpfer vein, the Rummel-Hoffer vein system in Banky, and the Ján Benedikty vein in Vyhne.

In summary, this work brings new data for the epithermal occurrences in the precious metal vein system in the central zone of the Štiavnica stratovolcano, related to the horst uplift. Some of the occurrences are simple in terms of their textures, hydrothermal breccias with quartz cement and weak ore mineralization. Other occurrences record hydrothermal activity in a complex, dynamic environment. Apart from fluid inclusions, a particular clue was found in the chemical composition of the carbonate minerals. This clue is definitely worth following if future work should be undertaken on these mineralizations.

Acknowledgements. We are thankful to P. Dobeš and M. Chovan for constructive reviews and comments that improved the manuscript. This study was financially supported by the *Deutsche Forschungsgemeinschaft* grant MA 3927-11-1, by VEGA grant 1/0560/15, by AVVV grant 15-0083 and by the project 1503 financed by the Ministry of Environment of the Slovak Republic.

References

Bakos F., Chovan M., Bačo P., Bahna B., Ferenc Š., Hvožďara P., Jeleň S., Kamhalová M., Kaňa R., Knésl J., Krasnec Ľ., Križáni I., Maťo Ľ., Mikuš T., Pauditš P., Sombathy L. & Šály J., 2004: Gold in Slovakia. Slovenský skauting, Bratislava, 298 p. [in Slovak with English summary]

Bergfest A., 1954: *Hodruša I*. Unpublished Report, Geological Institute of Dionýz Štúr in Bratislava, 105 p. [in Slovak]

Berkh K., Majzlan J., Chovan M., Kozák J. & Bakos F., 2014: Mineralogy of the Medieval Ag-Au occurrences Banská Belá, Treiboltz, Rabenstein, and Kopanice in the Banská Štiavnica ore district (Slovakia). *Neues Jahrbuch für Mineralogie, Abhandlungen*, 191, 237–256.

Bodnar R.J., Reynolds T.J. & Kuehn C.A., 1985: Fluid inclusion systematics in epithermal systems. *Reviews in Economic Geology*, 2, 73-98.

Bodnar R.J., 2003: Introduction to aqueous-electrolyte fluid systems. *In:* Samson, I., Anderson, A. & Marshall, D. (Eds.): Fluid Inclusions: Analysis and Interpretation. *Mineralogical Association of Canada, Short Course Series*, 32, 81–99.

Bodnar R.J., 1993: Revised equation and table for determing the freezing point depression of H_2O–NaCl solutions. *Geochimica et Cosmochimica Acta*, 57, 683–684.

Dong G., Morrison G. & Jaireth S., 1995: Quartz textures in epithermal veins, Queensland - Classification, origin and implication. *Economic Geology*, 90, 1841–1856.

Dove P.M. & Rimstidt J.D., 1994: Silica-water interactions. *In:* Heaney, P.J., Prewitt, C.T. & Gibbs, G.V. (Eds.): Silica. *Reviews in Mineralogy*, 29, 259–308.

Friedman I. & O´Neil J.R., 1977: Compilation of stable isotope fractionation factors of geochemical interest. *United States Geological Survey Professional Paper*, 440-KK.

Gašparek Ľ., 2009: Porovnanie vývoja žilných hydrotermálnych systémov Schöpfer a Trojkráľová v centrálnej zone štiavnického stratovulkánu. [A comparison of the development of vein hydrothermal systems Schöpfer and Trojkráľová in the central zone of the Štiavnica stratovolcano]. Unpublished Diploma thesis, Comenius University, Bratislava, 78 p. [in Slovak]

Harazim S., 1955: Záverečná správa a výpočet zásob Hodruša Au-Ag, stav k 1.1.1955. [Final report and reserve calculation in Hodruša Au-Ag as of January 1, 1955]. Unpublished manuscript, Geofond Bratislava. [in Slovak]

Kaňa R., Čelko M. & Mrákava F., 2011: Hodruša v zemi baníkov. [Hodruša in the miners' land]. Banskoštiavnický a hodrušský banícky spolok v Banskej Štiavnici, 192 p. [in Slovak]

Koděra M., 1959: Doterajšie výsledky výskumu parageneticých pomerov rudných žíl v štiavnicko - hodrušskom rudnom obvode. [The state of knowledge and research of the paragenetic relations in the Štiavnica-Hodruša ore district]. *Acta Geologica et Geographica Universitatis Comenianae*, 2, 7–17. [in Slovak with Russian and German summary]

Koděra M., 1960: Paragenetický a geochemický výskum Všechsvätých žily v Hodruši. [Paragenetic and geochemical exploration of the Všechsvätých vein in Hodruša]. *Acta Geologica et Geographica Universitatis Comenianae, Geologica, 4, 69-105*. [in Slovak]

Koděra M., 1969: On the relationship of Štiavnica and Hodruša ore-districts. *Mineralia Slovaca*, 1, 247–250. [in Slovak with English summary]

Koděra M. (Ed.): Topographic mineralogy of Slovakia. Veda, the Publishing House of Slovak Academy of Sciences, 1590 p. [in Slovak with English preface and introduction]

Koděra P., Lexa J., Rankin A.H. & Fallick A.E., 2005: Epithermal gold veins in a caldera setting: Banská Hodruša, Slovakia. *Mineralium Deposita*, 39, 921–943.

Koděra P., Lexa J., Konečný P., Ferenc Š., Maťo Ľ. & Hók J., 2007: Zdroje fluíd a genéza epitermálnych mineralizácií neovulkanitov. [Fluid sources and origin of the epithermal mineralization in Negene volcanic rocks]. Unpublished Report, State Geological Institute of Dionýz Štúr in Bratislava, 150 p. [in Slovak]

Koděra P., Lexa J., Fallick A.E., Wälle M. & Biroň A., 2014: Hydrothermal fluids in epithermal and porphyry Au deposits in the Central Slovakia Volcanic Field. *Geological Society, London, Special Publications*, 402, 177–206.

Kovalenker V.A., Naumov V.B., Prokof'ev V.Yu., Jeleň S. & Háber M., 2006: Compositions of magmatic melts and evolution of mineral-forming fluids in the Banská Štiavnica epithermal Au–Ag–Pb–Zn deposit, Slovakia: A study of inclusions in minerals. *Geochemistry International*, 44, 118–136.

Lexa J., Koděra P., Onačila D., Rojkovičová Ľ., Žáková E. & Tréger M., 1997: Komplexné hodnotenie prognóznych zdrojov nerastných surovín v oblasti centrálnej zóny štiavnického stratovulkánu, čiastková záverečná správa. [Complex evaluation of raw materials resources in the region

of the central zone of the Štiavnica stratovolcano]. Unpublished Report, Geological Institute of Dionýz Štúr in Bratislava, 233 p. [in Slovak]

Lexa J., Štohl J. & Konečný V., 1999: The Banská Štiavnica ore district: relationship between metallogenetic processes and the geological evolution of a stratovolcano. *Mineralium Deposita*, 34, 639–654.

Majzlan J., 2009: Ore mineralization at the Rabenstein occurrence near Banská Hodruša, Slovakia. *Mineralia Slovaca*, 41, 45–54.

Onačila D. & Rojkovičová Ľ., 1989: Nové poznatky o charaktere žily Trojkráľová v priestore považanskej poruchy. Správy o výskumoch GÚDŠ. [New information about the nature of the vein Trojkráľová near the Považany fault zone. Research reports of GUDŠ]. Geological Institute of Dionýz Štúr in Bratislava 25, 201-202. [in Slovak]

Onačila D. & Rojkovičová Ľ., 1992: Precious metal mineralization on the Hodruša ore field veins. *Mineralia Slovaca*, 24, 245–256. [in Slovak with English summary]

Onačila D., Rojkovičová Ľ., Žáková E., Repčok I., Eliáš K., Ferenčíková E., Harčová E., Hašková A., Kovárová A., Rúčka I. & Kalinaj M., 1993: Epitermálna žilná mineralizácia Hodrušského rudného poľa. [Epithermal vein mineralization of the Hodruša ore field]. Unpublished Report, Geological Institute of Dionýz Štúr in Bratislava, 142 p. [in Slovak]

Roedder E., 1984: Fluid inclusions. *Reviews in Mineralogy*, 12, 644 p.

Shepherd T.J., Rankin A.H. & Alderton D.H.M., 1985: A practical guide to fluid inclusion studies. Blackie and Son, London, 235 p.

Štohl J., Lexa J., Konečný V., Miháliková A., Onačila D., Hojstričová V., Žáková E., Brlay A., Rojkovičová Ľ. & Marsina K., 1986: Etapová správa za rok 1986 – Metalogenetický výskum centrálnej zóny štiavnického stratovulkánu. [Annual report for the year 1986 - Metalogenetic research of the central zone of the Štiavnica stratovolcano]. Archive of Geological Institute of Dionýz Štúr in Bratislava. [in Slovak]

Zrůstek V., 1957: Příspěvek k paragenesi a petrografii rudních žil v Hodruši. [Contribution to the parageneses and petrography of the ore veins in Hodruša]. *Geologické Práce, Zošit* 47, 159–194. [in Czech, with Russian and German Summary]